SWITCHED RELUCTANCE MOTOR DRIVE SYSTEMS DYNAMIC PERFORMANCE PREDICTION UNDER INTERNAL AND EXTERNAL FAULT CONDITIONS

A.A. Arkadan, Senior Member **B.W. Kielgas, Student Member**

Electrical and Computer Engineering Department
Marquette University
Milwaukee, WI 53233-2286

Abstract: In this second of a set of two companion papers on the dynamic performance of switched reluctance motor drive systems, the results of using an iterative approach to predict the dynamic performance characteristics of a motor drive system during fault conditions are presented. The method is applied to a 6/4, 0.15 hp, 5000 r/min switched reluctance motor drive system to study an external fault due to the failure of a transistor in the converter. The model is also used to study an internal fault due to a partial armature phase short. The analysis resulted in the performance characteristics of the motor drive system which are verified by comparison to experimental data. In addition, the effects of mutual coupling between motor phases on the analysis results are evaluated.

Keywords:
Switched Reluctance Motor Drive Systems
Iterative Inductance Updating Approach
Internal and External Fault Analysis

INTRODUCTION

The significance of the accurate performance prediction of fault tolerant switched reluctance motor (SRM) drive systems can best be considered by looking at important current and potential applications. This class of motors is already used in high performance applications including incremental motion control and adjustable speed drive systems. In addition, this class of motors is being considered for use in critical aerospace applications such as actuators and compressor systems where it is required that the system operate reliably despite partial failures. In a recent work by Stephens [1], internal and external fault conditions were examined on a particular drive system, but the analysis involved only experimental results. The computer aided modeling of both internal and external faults has been documented on other types of machines [2-9]. In the work of Arkadan et al [2-4] a method for modeling permanent magnet generators was presented and external faults in the electronic components were considered. This included the effects of harmonics in the machine currents due to material nonlinearities and power electronic component switching. However, the speed was assumed to be constant due to the high inertia of the rotor, and the winding inductance values were not updated during the fault period. In the work of Kulig et al, [5-7], a model to study effects of circuit asymmetries due to internal faults in synchronous generators was developed. However saturation was not accounted for in all parts of the machine, and nonlinearities due to external circuits were not studied, and machine inductance values were not updated throughout the analysis. Meanwhile, in the work of Nyamousa and Demerdash [8,9], internal faults were considered and machine winding inductance values were updated during a fault condition. However, the speed was assumed constant, external faults in associated power electronics were not considered, and harmonics due to switching electronics were not fully accounted for. In this work, the approach presented in a companion paper [10] to predict the dynamic performance characteristics of SRM drive systems under normal operating conditions is extended to study faults. Using this approach, the effects of harmonics in the machine currents due to power electronic switching, changes in motor speed, as well as magnetic material nonlinearities and space harmonics due machine geometry are accounted for when predicting the performance characteristics of the SRM drive system during internal and external fault conditions. Furthermore, an iterative approach is used to update the inductances during the fault conditions to account for the change in magnetic material saturation of the SRM and the speed during the fault condition. A convergence criterion based on the simulated speed of the SRM is used as a check for convergence. The two faults considered are that of an external transistor failure resulting in an open circuit and an internal partial armature phase short. In addition, the analysis results are compared with test data for verification.

93 WM 026-5 EC A paper recommended and approved by the IEEE Electric Machinery Committee of the IEEE Power Engineering Society for presentation at the IEEE/PES 1993 Winter Meeting, Columbus, OH, January 31 - February 5, 1993. Manuscript submitted September 1, 1992; made available for printing December 14, 1992.

SWITCHED RELUCTANCE MOTOR DRIVE SYSTEM AND STATE SPACE MODEL DESCRIPTION

As was detailed in the companion paper [10], the SRM drive system considered in this work consists of the SRM itself, an inverter used to supply power to the motor, a controller used to control the switching of the inverter, and a hysteresis brake used to load the motor. The SRM utilized for the analysis is a 6/4 machine rated at 0.15 hp at 5000 r/min. A cross section of the machine is shown in Figure (1). The coils of diametrically opposite stator poles are connected in series to aid each other and to form one phase of the machine. The motor consists of three phase windings designated as (a), (b), and (c). The inverter configuration used for this analysis is shown in Figure (2). A constant speed controller was developed which used position feedback from an optical encoder to switch the motor phases every 30°. In addition, the offset of the switching from a fixed reference was also controlled. For full details, reference [11] should be consulted.

The lumped parameter state space model for the dynamic analysis of SRM's, was presented in a companion paper [10] and is given here for continuity:

$$\underline{V} = \underline{R}\,\underline{I} + \underline{L}\frac{d\underline{I}}{dt} + \omega_m \frac{d\underline{L}}{d\theta}\underline{I} \tag{1}$$

where the matrix $\underline{L}$ represents the SRM self and mutual inductance and is given as follows:

$$\underline{L} = \begin{bmatrix} L_{aa} & L_{ab} & L_{ac} \\ L_{ba} & L_{bb} & L_{bc} \\ L_{ca} & L_{cb} & L_{cc} \end{bmatrix} \tag{2}$$

The mutual inductances are included in the analysis in order to determine their effect on predicting the system performance. The array $\underline{V}$ represents the SRM phase voltages, v_a, v_b, and v_c. The array $\underline{I}$ represents the phase currents, i_a, i_b, and i_c, and the matrix $\underline{R}$ represents the machine phase resistances. In addition, the effect of the electromechanical torque on the state model is determined by incorporating the relationship:

$$\frac{d\omega_m}{dt} = \frac{1}{J}(T_{em} - B\omega_m - T_L) \tag{3}$$

where ω_m is the rotor speed in radians per second, J is the inertia of the rotor, T_{em} is the developed electromechanical torque, B is the coefficient of viscous friction, and T_L is the load torque. The developed torque was calculated using the well known relationship $T_{em} = \frac{P}{\omega_m}$ where $P = ei$, and e is the rotational voltage which is the last term of Equation (1).

The values of the currents i_a, i_b, and i_c, of equation (1), and the rotor speed, ω_m, of equation (2) can be determined numerically for any set of initial conditions and terminal voltages v_a, v_b, and v_c. The method used in determining the inductances of the state space model from nonlinear magnetic field solutions to predict the SRM drive system performance under normal operating conditions was described in the companion paper [10]. In this paper, these parameters are updated during fault conditions as described next.

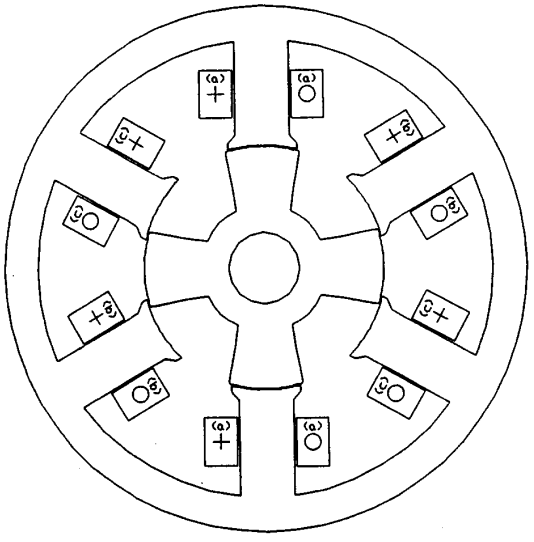

Figure (1): Motor Cross Section

AN ITERATIVE APPROACH

In simulating the faulted operation of the motor, an iterative approach is used in order to update the inductances during the fault condition. Another iterative inductance updating approach was used by Demerdash and Baldassari [12,13] in order to predict the steady state performance of an induction motor. However, no external electronic circuits were involved an the analysis, and fault conditions were not examined. In addition, the motor speed was assumed constant and the convergence criterion adopted involved the use of machine currents. The approach outlined in this work uses the original steady state (before fault) inductances and simulates an internal or external fault. The state space model is then run until it reaches a faulted steady state condition. The currents from this analysis are then used in the finite element model to predict a new set of updated inductances. These updated inductances are then used in the state model to predict a new set of fault currents. This approach is repeated until a convergence criterion is satisfied. A flowchart outlining this approach is shown in Figure (3).

As for the convergence criterion used in the model, the change in the normalized rotor speed is checked against a convergence tolerance. In other words, the speed computed in the state model is utilized as the criterion for convergence during the fault condition. The normalized speed change from one iteration to the next iteration is as follows:

$$\frac{\omega_i - \omega_{i+1}}{\omega_{ss}} \leq \epsilon \tag{4}$$

where ω_i is the speed at iteration i, ω_{i+1} is the speed at iteration $i+1$, and ω_{ss} is the steady state speed prior to the onset of the fault. If the value for equation (3) is less than ϵ, where ϵ is a convergence tolerance, the resulting fault condition is considered to have converged. The results of implementing this approach to predict the SRM drive system performance characteristics in the case of an external fault due to a transistor failure resulting in opening of a motor phase and in the case of an internal fault resulting in partial armature phase short, are presented below. It should be noted here that only three iterations were needed to reach convergence for each of the fault cases investigated in this work.

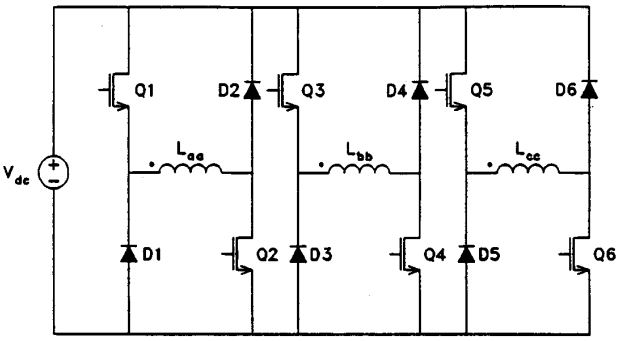

Figure (2): Inverter Configuration

PHASE TRANSISTOR FAILURE CONDITION

The results of modeling a solid state component failure in the inverter are presented. In this case, a transistor failure resulting in a sustained open circuit in phase (b) is studied. The inverter is shown in Figure (2), and the phase transistor Q_3 is modeled as an open in the analysis. Initially, the steady state (before fault) inductance profiles are used, which are determined using the approach outlined in the companion paper [10]. The inductances are then updated with the approach outlined above during a fault condition. The performance characteristics of the SRM drive motor system were predicted for this external fault at no load and load conditions and are given below.

No Load Case:

The state space model and the approach described above for updating the inductances was used to predict the performance characteristics of the SRM drive system during a phase transistor failure condition at no load. Based on this approach, the self and mutual inductance values were updated during the fault condition. The calculations were carried out by stepping the rotor by 2^o mechanical increments and performing a nonlinear field solution to cover a complete cycle of the SRM operation. This is repeated during each iteration of the procedure shown by the flowchart, Figure (3). The computer simulated profiles (CSP's) of the current for an unfaulted (healthy) phase and the SRM developed torque are shown by the solid lines in Figures (4) and (5), respectively. In addition, the profile of the measured phase current for an unfaulted phase is shown in Figure (6). The CSP and the measured waveform for the faulted phase (b) current are not shown as they have a zero value.

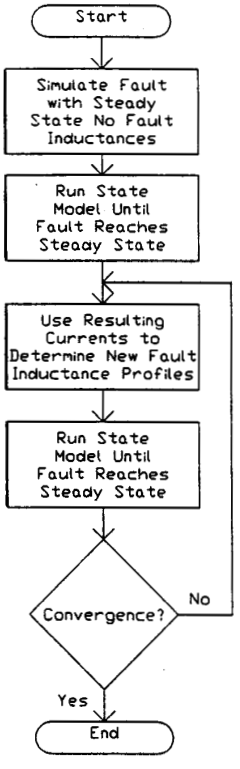

Figure (3): Flowchart of Iterative Fault Inductance Calculation

An inspection of the CSP of the unfaulted phase current at no load, Figure (4), and the corresponding measured values, Figure (6) reveals the good agreement and verifies the validity of this modeling approach. In addition, an inspection of the CSP of the developed torque, Figure (5), shows the effects of opening of the armature phase due to the transistor failure. The dips in the torque profile of Figure (6), correspond to the periods phase (b) is unable to conduct due to the fault, as one expects.

Further results are given in Table (1) as obtained from simulations and measurements. Table (1) shows the values of the unfaulted phase (a) current, developed torque, and speed during the sustained fault as well as prior to the onset of the fault. The pre fault values are given in brackets, (), as obtained from simulations and measurements.

An examination of the values in Table (1) reveals an increase in the current values of the healthy phase (a) due to the opening of phase (b). This is due to both the decrease in speed during the fault condition which allows each phase to be 'on' for a longer period of time and the decrease in rotational voltage which opposes the current rise. Also it should be pointed out that the average values of the developed torque and speed are reduced during the fault period, as is shown in Table (1). This is expected, since the three phase SRM is now operating with only two phases. It should be pointed out also that the measured value for the torque needed to overcome friction and windage is not available (N/A). The numerical comparison results provided in Table (1) show the good agreement between the simulated and measured values. These results further confirm the validity of this modeling approach.

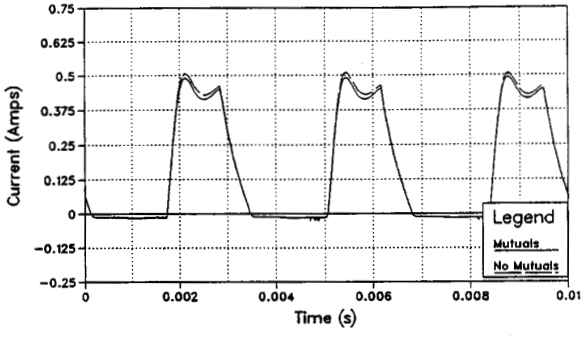

Figure (4): Simulated Current Profile for an Unfaulted Phase During a Transistor Failure in Phase (b) at No Load

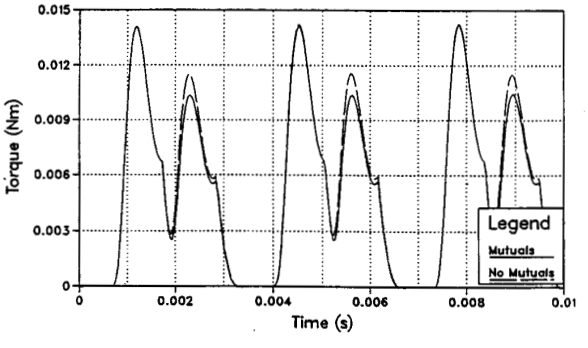

Figure (5): Simulated Developed Torque with Transistor Failure in Phase (b) at No Load

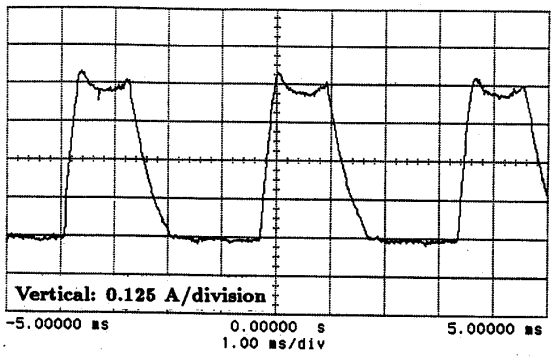

Figure (6): Measured Unfaulted Phase Current During a Transistor Failure in Phase (b) at No Load

Transistor Fault at No Load		
	Simulated	Measured
	Fault (Pre Fault)	Fault (Pre Fault)
$I_a(dc) - A$	0.166 (0.150)	0.183 (0.152)
$I_a(rms) - A$	0.197 (0.180)	0.213 (0.175)
Torque (Avg.)- Nm	0.005 (0.006)	N/A (N/A)
Speed (Avg.) - rad/s	472.7 (523.7)	436.3 (523.6)

Table 1: Comparison of Simulated and Test Data with Transistor Failure at No Load

1.0 Per Unit Load Case:

Next, the state space model and the approach described previously for updating the inductances was used to predict the performance characteristics of the SRM drive system during a phase transistor failure condition during the 1.0 per unit (p.u.) load condition at a speed of 2500 r/min. Based on this approach, the self and mutual inductance values were updated during the fault condition and this resulted in the performance characteristics of the SRM drive system at 1.0 p.u. load condition. The CSP's for the current of the unfaulted phase (a) and the developed torque are shown by the solid lines in Figures (7) and (8), respectively, for this 1.0 p.u. load condition. In addition, the measured current waveform for an unfaulted phase is shown in Figure (9). Additional results are provided in Table (2).

Again, an inspection of the phase current profiles as obtained from simulations, Figure (7), and measurements, Figure (9), and the numerical comparison of the results given in Table (2), reveals the good agreement and further demonstrates the validity of this modeling approach. Furthermore an examination of the results in Table (2) shows an increase in the unfaulted phase current. Again, this is due to the decrease in speed during the fault condition which allows each phase to be 'on' for a longer period of time, the decrease in rotational voltage which opposes the current rise, and the decrease in the inductance value during the faulted condition due to saturation. In addition, it should be pointed out that the average value of the developed torque and speed is reduced during the fault period, as is shown in Table (2), and Figure (8). This is expected, since the three phase SRM is now operating with only two phases. Also it should be noted here that the discrepancy between the simulated and measured torque values in Table (2) can be attributed to the fact that the measured value for the torque reflects the value of the applied load (hysteresis brake) only and does not include the torque needed to overcome friction and windage in the SRM, while the computed value accounts for both.

In addition, a separate model was run neglecting the mutual inductances for both the no load and 1.0 p.u. load cases in order to determine their effect on the simulation results during the fault condition. The results for the analysis neglecting the mutual inductances are shown by the dashed lines in Figures (4) and (5) for the no load case, and Figures (7) and (8) for the load case. An examination of these figures reveals that there was no significant effect due to the mutual coupling between phases. This can be accounted for by noting that only one phase of the SRM is 'on' at any one time.

As was demonstrated above, a very good agreement exists between the measured values and simulated results for the external fault condition. Accordingly, the developed models are validated and the work is extended to study the case of an internal fault resulting in a partial armature phase short condition. The simulated results are outlined in the following section. It should be stated that no test data is available for this case because the motor was constructed without any provisions for access to the machine phase windings.

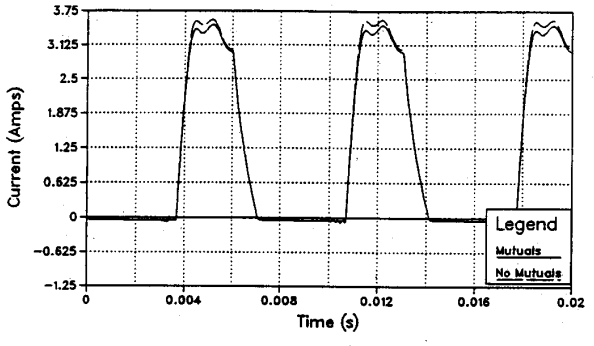

Figure (7): Simulated Current Profile for an Unfaulted Phase During a Transistor Failure in Phase (b) at 1.0 P.U. Load

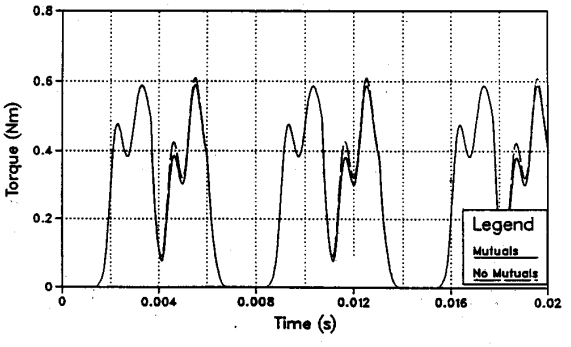

Figure (8): Simulated Developed Torque with Transistor Failure in Phase (b) at 1.0 P.U. Load

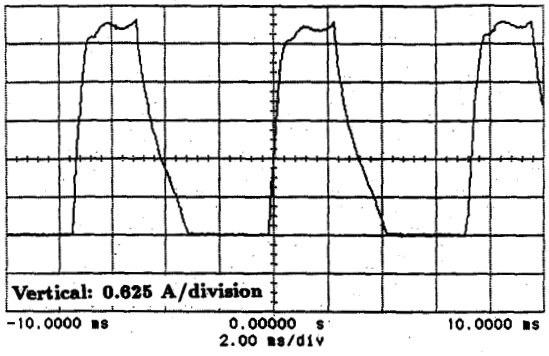

Figure (9): Measured Unfaulted Phase Current During a Transistor Failure in Phase (b) at 1.0 P.U. Load

Transistor Fault at Load		
	Simulated	Measured
	Fault (Pre Fault)	Fault (Pre Fault)
$I_a(dc) - A$	1.110 (0.969)	1.280 (1.080)
$I_a(rms) - A$	1.450 (1.220)	1.400 (1.170)
Torque (Avg.)- Nm	0.248 (0.253)	0.217 (0.217)
Speed (Avg.) - rad/s	223.3 (261.8)	212.3 (261.8)

Table 2: Comparison of Simulated and Test Data with Transistor Failure at 1.0 P.U. Load

PARTIAL ARMATURE PHASE SHORT CONDITION

In this section, the results of modeling an internal fault due to a partial armature phase short condition are presented. As mentioned earlier, each phase is formed by connecting diametrically opposite stator poles in series. In the case under study, a short is assumed to take place across one of the poles of phase (b), Figure (1), thus resulting in shorting half the turns of phase (b) coil. The results are given here for a 1.0 p.u. load condition. Using the iterative approach outlined in this paper, the self and mutual inductance values were updated for this internal fault condition. This resulted in the performance characteristics for the SRM drive system under consideration.

The advantage of the iterative inductance updating approach can best be considered by examining the inductance values determined for this partial armature fault condition. Based on conventional theory [14], at the onset of the fault condition, the average value of the self inductance of the faulted phase was considered to be at half its original value that existed before the onset of the fault. This is the case, since a half the number of turns are assumed to be shorted in this fault case. However, based on this iterative approach, which was validated earlier in this paper, it was found that the self inductance L_{bb}, for the faulted phase (b), has an updated average value which is at 39% of the original value that existed before the fault. Meanwhile, in the case of the mutual inductances, the average value of the updated mutual inductance L_{ab} was found at 45% of the original value before the fault. This can be attributed to the magnetic saturation effects that are accounted for in the modeling approach.

The CSP's of the current of an unfaulted phase, the current of faulted phase (b), and the developed torque are given by the solid lines in Figures (10) through (12), respectively. In addition, a summary of the performance characteristics are given in Table (3), as obtained prior to the onset of the fault and during the sustained fault condition.

Examining the values in Table (3) as well as the CSP of an unfaulted phase current in Figure (10) reveals the decrease in the unfaulted phase current values in comparison to the pre fault values. This is due to both the increase in speed during the fault condition which allows each phase to be 'on' for a shorter period of time and the increase in rotational voltage which opposes the current rise. However, an examination of the CSP of the faulted phase (b) current, Figure (11), and corresponding current values in Table (3) shows almost a doubling of the faulted phase (b) current values during this internal fault condition. Again, this is expected due to the reduction in the inductance values as was mentioned earlier. Also, it should be pointed out that an inspection of the CSP of the developed torque, Figure (12), and the numbers in Table (3), shows the increase in the average values of the developed torque and speed during the sustained fault condition. This is expected, because of the increase in the value of the current in the faulted phase (b) and since the torque is proportional to the square of the value of the phase currents.

Again, a separate model was run neglecting the mutual inductances in order to determine their effect on the analysis results for this fault

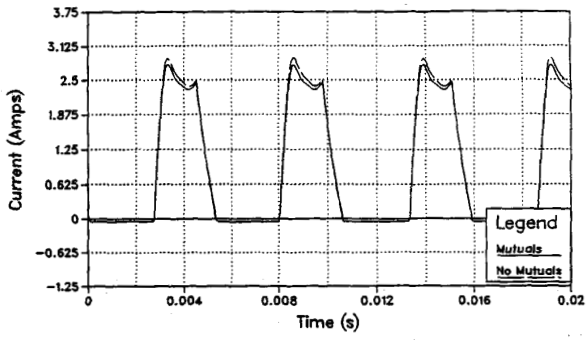

Figure: (10): Unfaulted Phase Simulated Current with Partial Armature Short in Phase (b) at 1.0 P.U. Load

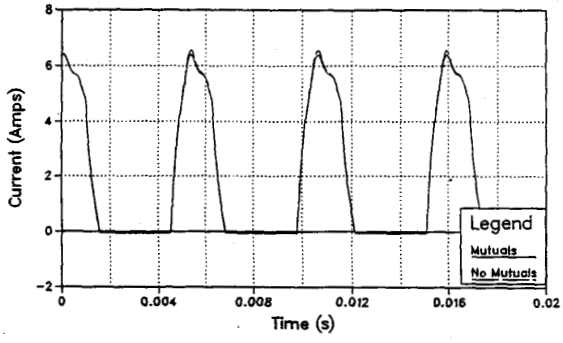

Figure (11): Faulted Phase Simulated Current with Partial Armature Short at 1.0 P.U. Load

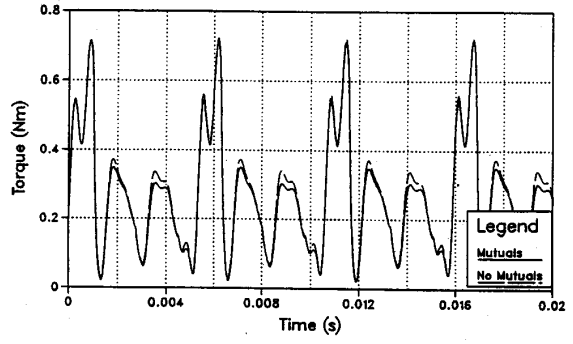

Figure (12): Simulated Developed Torque with Partial Armature Short in Phase (b) at 1.0 P.U. Load

condition. The results for the analysis neglecting the mutual inductances are shown by the dashed line in Figures (10) through (12). An examination of these figures reveals that one can neglect the mutual coupling between the phases of the SRM model without significantly affecting the simulation results for the motor drive system under consideration. This can again be accounted for by noting that only one phase of the machine is 'on' at one time, and relatively low levels of current exist in a phase during the regeneration period following the instant the transistors are turned off for that phase. However, it should be noted here that other control strategies are used with SRM drive systems where it is required to excite two phases simultaneously for a period of time. In such cases it is expected that the inclusion of the mutual inductances in the simulation model would lead to more accurate results.

It should be pointed out, that the results obtained for this external fault condition show a doubling in the peak value of the faulted phase and an unbalance in the developed torque profile in comparison to normal operating conditions [10]. This unbalance in the torque profile and the doubling of the unfaulted phase current is due to the unbalanced operating conditions and could present problems for some applications. However, the ability of the SRM to produce torque during this internal fault condition, as well as during the external fault condition discussed earlier, could be of interest in some aerospace applications. In such applications, it is required that the system operate reliably despite partial failures.

Finally, it should be noted that this modeling approach has been verified based on experimental results given in this paper as well as in the companion paper [10]. Accordingly, it can be stated that this approach, which is general in nature, can be used to study the fault tolerance of other inverter configurations. In addition, based on such studies, fault handling control strategies could be developed and optimized to minimize the effects of partial failures on the performance characteristics of SRM drive systems.

Partial Armature Short at 1.0 P.U. Load		
	Pre Fault	Fault
$I_a(dc)A$	0.969	0.845
$I_a(rms)A$	1.220	1.070
$I_b(dc)A$	0.969	1.760
$I_b(rms)A$	1.220	2.440
Torque (Avg.) Nm	0.253	0.258
Speed (Avg.) rad/s	261.8	297.3

Table 3: Simulated Data of Partial Armature Short at 1.0 P.U. Load Condition

CONCLUSION

The results of using an iterative approach to predict the dynamic performance characteristics of an SRM drive system during fault conditions were presented. The method is applied to a 6/4, 0.15 hp, 5000 r/min switched reluctance motor drive system to study external and internal fault conditions. The analysis resulted in the performance characteristics of the motor drive system which were verified by comparison to experimental data. Based on the analysis, it was demonstrated that the effects of mutual coupling between motor phases can be neglected from the analysis for this class of SRM drive systems. In addition, based on the simulation and measured data it was shown that SRM drive system under consideration is capable of producing torque under partial fault conditions. Accordingly, it can be concluded that this modeling approach, which is general in nature, can be used to study the fault tolerance of other SRM drive systems as well as to develop fault handling control strategies to minimize the effects of partial failures on the motor torque and speed.

References

[1] Stephens, C.M., "Fault Detection and Management System for Fault Tolerant Switched Reluctance Motor Drives," *Conference Record of the IAS Annual Meeting pt 1*, pp. 574-578, 1989.

[2] Arkadan, A.A., Demerdash, N.A., Vaidya, J.G., and Shah, M.J., "Impact of Load on Winding Inductances of Permanent Magnet Generators with Multiple Damping Circuits Using Energy Perturbation," *IEEE Transactions on Energy Conversion*, vol. EC-3, No. 4, pp. 880-889, 1988.

[3] Arkadan, A.A., and Demerdash, N.A., "Modeling of Transients in Permanent Magnet Generators with Multiple Damping Circuits Using the Natural abc Frame of Reference," *IEEE Transactions on Energy Conversion*, vol. EC-3, No.3, pp. 722-731, 1988.

[4] Arkadan, A.A., Hijazi, T.M., and Demerdash, N.A., "Computer-Aided Modeling of a Rectified DC Load Permanent Magnet Generator System with Multiple Damper Windings in the Natural abc Frame of Reference," *IEEE Transactions on Energy Conversion*, vol. EC-4, No. 3, pp. 518-525, 1989.

[5] Kulig, T.S., Buckley, G.W., Lambrecht, D., and Liese, M., "A New Approach To Determine Generator Winding and Damper Currents In Case of Internal and External Faults and Abnormal Operation. Part I: Fundamentals, Paper No. 87 WM 203-3, *IEEE-PES* Winter Meeting, New Orleans, Feb. 1-6, 1987.

[6] Kulig, T.S., Buckley, G.W., Lambrecht, D., and Liese, M., "A New Approach To Determine Generator Winding and Damper Currents In Case of Internal and External Faults and Abnormal Operation. Part II: Analysis," Paper No. 87 WM 204-1, *IEEE-PES* Winter Meeting, New Orleans, Feb. 1-6, 1987.

[7] Kulig, T.S., Buckley, G.W., Lambrecht, D., and Liese, M., "A New Approach To Determine Generator Winding and Damper Currents In Case of Internal and External Faults and Abnormal Operation. Part III: Results, *IEEE Transactions on Energy Conversion*, vol. EC-5, No.1, pp. 70-78, 1990.

[8] Nyamusa, T.A., Demerdash, N.A., "Integrated Nonlinear Magnetic Field-Network Simulation of an Electronically Commutated Permanent Magnet Motor System Under Normal Operating Conditions," *IEEE Transactions on Energy Conversion*, vol. EC-1, No. 1, pp. 77-85, 1987.

[9] Nyamusa, T.A., Demerdash, N.A., "Transient Analysis of Partial Armature Short Circuit in an Electronically Commutated Permanent Magnet Motor System Using an Integrated Nonlinear Magnetic Field-Network Model," *IEEE Transactions on Energy Conversion*, vol. EC-1, No. 1, pp. 86-92, 1987.

[10] Arkadan, A.A., and Kielgas, B.W., "Switched Reluctance Motor Drive Systems Dynamic Performance Prediction and Experimental Verification," A companion Paper Submitted for Presentation at the 1993 IEEE-PES, Winter Meeting, Columbus, Ohio.

[11] Kielgas, B.W., "Computer-Aided Analysis of Fault Tolerant Switched Reluctance Motor Drive Systems," Master's Thesis, Marquette University, August 1992.

[12] Demerdash, N.A., and Baldassari, P.,"A Combined Finite Element-State Space Modeling Environment for Induction Motors in the abc Frame of Reference: The No-Load Condition," *IEEE Transactions on Energy Conversion*, vol. EC-7, No. 4, pp. 698-709, 1992.

[13] Baldassari, P., and Demerdash, N.A.,"A Combined Finite Element-State Space Modeling Environment for Induction Motors in the abc Frame of Reference: The Blocked-Rotor and Sinusoidally Energized Load Condition," *IEEE Transactions on Energy Conversion*, vol. EC-7, No. 4, pp. 710-720, 1992.

[14] Fitzgerald, A.E., Kingsley, C., and Umans, S.D., *Electric Machinery*, 4th Edition, McGraw Hill Book Company, 1983.

Abdul-Rahman A. Arkadan (S-79, M-88, SM-91) received his B.S. degree from the University of Mississippi in 1980, his M.S. degree from Virginia Polytechnic Institute in 1981, and his Ph.D. degree from Clarkson University in 1988, all in electrical engineering. During the period 1981-1984 he worked in industry. In 1988, he joined the Department of Electrical and Computer Engineering at Marquette University as an Assistant Professor. His interests include design, analysis, and development of electronically-operated machine systems and drives, and computer-aided solution of electromagnetic field problems in electromagnetic devices. He is a member of ASEE, Sigma XI, Phi Kappa Phi, Pi Mu Epsilon, Eta Kappa Nu, Tau Beta PI, and a Registered Professional Engineer in the State of Wisconsin. Dr. Arkadan is a senior member of the IEEE and a member of the IEEE-PES Electric Machinery Committee (EMC) and the IEEE-PES Education Committee. He is the Secretary for the IEEE-PES-EMC Direct Current, Permanent Magnet and Special Machines Subcommittee and a member in several of IEEE-PES subcommittees and working groups.

Bruce W. Kielgas (S-92) received his B.S. degree in electrical engineering from Marquette University in 1990. Also he received his M.S. degree in electrical engineering from Marquette University in August 1992 where he was working in the development of computer models to predict the dynamic performance characteristics of SRM drive systems under normal and fault conditions. Currently Mr. Kielgas is at Westinghouse Electric Corporation at Orlando Florida. His interests include finite element analysis of electromagnetic devices and the computer- aided simulation of power electronic systems. He is a member of IEEE and Tau Beta Pi.

Discussion

Nabeel A. O. Demerdash, Clarkson University, Potsdam, New York: The authors are to be congratulated on an interesting paper showing simulations of switched reluctance motor drives under unbalanced fault conditions. Table (2) shows an interesting condition in which the apparent loss of one phase leads to a reduction of the average torque of less than a few percent. One would normally expect a loss in torque magnitude of more than 34% when one phase is faulted in a 3 phase machine. Would the authors explain the reasons for such a limited drop in the average torque magnitude? If the degradation of the torque under faulted conditions is as limited as shown in the paper, such a drive system characteristic would be a considerable advantage in aerospace applications where safety and redundancy are very important deciding factors.

Manuscript received February 22, 1993.

A.A. Arkadan and B.W. Kielgas: These authors wish to express their thanks to Dr. Demerdash for his useful comments and interesting questions included in his discussion. In response to his question regarding the limited drop in the average torque magnitude due to a transistor failure, the authors offer the following. In the constant speed, closed loop control scheme utilized for the motor under discussion, each of the three phases is switched sequentially every 30° electrical. In the fault condition considered, one phase of the motor is removed from the system due to a transistor failure. When one phase is faulted, the speed of the machine is reduced. This, in turn, results in the two unfaulted phases remaining 'on' for a longer period of time than in the unfaulted case. This allows for a larger current value in each of the unfaulted phases. Accordingly, it results in greater electromechanical torque production in the two unfaulted phases as shown by equations (10) and (11) of the paper. In this case, it can be stated that the machine compensates for the loss of the faulted phase by producing more torque in the healthy (unfaulted) phases. However, a drawback to this phenomenon is that, during fault, the machine speed is reduced in comparison to its prefault value. This is confirmed in the paper, Table (2). Based on results obtained from simulations and measurements, the machine average speed value was reduced after the onset of the fault. Moreover, it should be noted that if the machine is to be used under such mode of operation (partial failure), the machine must be designed to withstand the higher levels of current in the healthy phases. In addition, the switching devices in the converter should be rated accordingly. In spite of that, the limited drop in the average torque magnitude in such a drive system could be advantageous in some aerospace applications where it is required that the system operates reliably despite partial failures.

Manuscript received April 8, 1993.